Journal of Applied Mechanics and Technical Physics, Vol. 47, No. 6, pp. 857–866, 2006

DISLOCATION STRUCTURE OF SHEAR BANDS IN SINGLE CRYSTALS

S. P. Kiselev

UDC 548.24

A mathematical model is proposed for the development of a shear band in crystals. The model is based on the mechanism of double cross-slips of screw-dislocation segments. Equations are derived to study instability of the uniform distribution of dislocations. A solution is found in the form of a traveling wave, which describes the shear-band structure.

Key words: *stresses, strain, dislocations, shear band.*

Introduction. Reaching the critical value of the shear stress is known to lead to plastic deformation of the crystal. Dislocation loops start moving in the shear plane and expanding, which results in emergence of shear bands [1]. As the strain increases, the shear bands can become packed into bunches, forming Lüders–Chernov slip bands at the macroscopic level [2]. Thus, slip bands play an important role in plastic deformation and are intensely studied both theoretically and experimentally.

Experimental data on shear bands in ionic LiF crystals with a face-centered cubic lattice can be found in [3]. The LiF crystal was chosen because plastic deformation at the initial stage in this crystal proceeds in one slip plane aligned at an angle of 45° to the extension (compression) axis. Expansion of the shear band is found to occur owing to double cross-slips of screw-dislocation segments. Crystal deformation occurs only at the shear-band front. Because of the action of internal stresses due to clustering of dislocations, their velocity behind the band front tends to zero, and the plastic strain inside the band remains constant. Mathematical models that describe shear-band expansion owing to the mechanism of double cross-slips were constructed in [4–6]. Under the assumption that the double cross-slips have a stochastic character, diffuse equations of the type of the Kolmogorov–Petrovskii–Piskunov–Fisher equation for dislocation density were derived in [4–6], and the solutions of these equations were examined. Implementation of the approach proposed in [4–6], however, has significant drawbacks: equations derived in [4] contain negative diffusion coefficients, which contradicts the second law of thermodynamics. The assumption on a constant velocity of dislocations made in [5, 6] contradicts experimental data on deceleration of dislocations inside the shear band [3]. The mathematical model of shear-band propagation constructed in the present work is devoid of the above-mentioned drawbacks; solutions that describe the structure of the shear band considered in [3] are obtained.

1. Derivation of Equations. We consider a planar sample extended along the x_1 axis under the action of stress σ_1. We assume that the motion of dislocations occurs in a slip plane inclined to the x_1 axis by an angle ψ (Fig. 1). Plastic deformation occurs owing to the motion of dislocation loops until their deceleration on obstacles of different origin (admixtures, effusion, etc.). Under the action of local stresses, the screw segment of the decelerated dislocation loop can be ejected into the neighboring slip plane to give rise to a Frank–Reed source, which generates dislocation loops moving in a parallel slip plane. In turn, the dislocation loop in the initial slip plane can turn around the obstacle and continue its motion. The time and distance of ejection of the screw segment have a random character, and the process of multiplication of dislocations has to be described by an integrodifferential kinetic balance equation (see [4]). It should be noted that, if the ejection distance is $h < h_0$, this segment does not move because of elastic interaction of the ejected segment with the dislocation in the initial plane, and two dislocation dipoles arise owing to ejection [3]. If $h > h_0$, the dislocation segment is expanded in the neighboring plane. As the

Khristianovich Institute of Theoretical and Applied Mechanics, Siberian Division, Russian Academy of Sciences, Novosibirsk 630090; kiselev@itam.nsc.ru. Translated from Prikladnaya Mekhanika i Tekhnicheskaya Fizika, Vol. 47, No. 6, pp. 102–113, November–December, 2006. Original article submitted December 26, 2005.

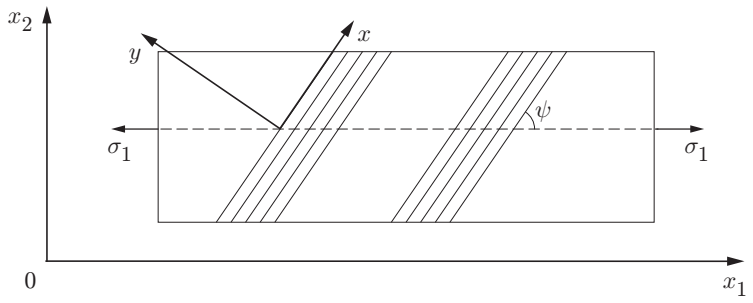

Fig. 1. Development of slip bands in a planar sample under uniaxial tension along the x_1 axis (dislocations move along the x axis, and slip bands expand in the y direction).

segment ends are fixed, the segment is a Frank–Reed source of dislocation loops whose motion leads to new acts of double cross-slips. The critical distance of segment ejection is determined by the formula [3]

$$h_0 = \mu b/(8\pi(1-\nu)(\sigma-\sigma_f)), \tag{1.1}$$

where μ is the shear modulus, ν is Poisson's ratio, b is the absolute value of the Burgers vector, σ is the shear stress, and σ_f is the dry friction stress. The number of negative dislocations is assumed to be equal to the number of positive dislocations; hence, Eq. (1.11) contains no far-range stresses described in [7].

Taking into account these comments, we write the integrodifferential equation for dislocation density [4]:

$$\frac{\partial\rho}{\partial t}+\frac{\partial\rho u}{\partial x}+\frac{\partial\rho v}{\partial y}=\int\limits_x^\infty Q(x'-x)R(y)\,dx'+f', \quad Q(x'-x)=\frac{1}{\lambda_s}\exp\Big(-\frac{|x'-x|}{\lambda_s}\Big),$$

$$\frac{\partial\rho_i}{\partial t}=\int\limits_x^\infty dx'\,Q(x'-x)\int\limits_{y-h_0}^{y+h_0}\frac{\rho'u'}{\lambda_s'}\,P(y'-y)\,dy'+\varphi', \quad P(y'-y)=\frac{1}{h_c}\exp\Big(-\frac{|y'-y|}{h_c}\Big), \tag{1.2}$$

$$R(y)=\int\limits_{-\infty}^{y-h_0}q_{\rm FR}\,\frac{\rho'u'}{\lambda_s'}\,P(y'-y)\,dy'+\int\limits_{y+h_0}^{\infty}q_{\rm FR}\,\frac{\rho'u'}{\lambda_s'}P(y'-y)\,dy'.$$

Here $u'=u(\rho')$, $\lambda_s'=\lambda_s(\rho')$, $\rho'=\rho(x',y')$, u and v are the components of velocity of dislocations in the x and y directions, respectively (see Fig. 1), ρ and ρ_i are the densities of moving and motionless dislocations, respectively, $q_{\rm FR}$ is the number of dislocation loops arising in the neighboring slip plane owing to the Frank–Reed mechanism, $Q(x'-x)$ is the probability that the screw segment of the dislocation loop runs the distance $x'-x$ after double cross-slips, $P(y'-y)$ is the probability of ejection of the screw segment to the distance $y'-y$, λ_s and h_c are the characteristic length of travel and ejection of the screw segment, f' and φ' are the terms that describe multiplication of moving and motionless dislocations, which are determined by the formulas [4]

$$f'=un-(\lambda_{is}^{-1}+h_i\rho_i)u\rho+\delta_f\rho_f u\rho-h_a u\rho^2, \qquad \varphi'=-h_d\rho_i u\rho, \tag{1.3}$$

λ_{is} is the distance covered by the screw segments of the dislocation loop before they stop on obstacles of the non-deformation nature, n is the concentration of the Frank–Reed sources, h_i is the size of dislocation dipoles decelerating moving dislocations, h_a is the distance at which annihilation of dislocations of the opposite sign occurs, h_d is the size of dislocation dipoles destroyed by moving dislocations, and $\delta_f\approx 10^{-2}$ is a constant. The first term in the right side of the first equation in (1.3) describes multiplication of moving dislocations by the Frank–Reed sources, the second term describes termination of dislocation motion on obstacles and dipoles, the third term describes multiplication of moving dislocations on forest dislocations ρ_f, and the fourth term describes annihilation of dislocations. In the second equation of (1.3), the term in the right side describes the destruction of dislocation dipoles by moving dislocations. If the dislocation motion has a thermally activated character, the dislocation velocity in the slip plane is approximated by the formula [3]

$$u = u_0\Big(\frac{\sigma - \sigma_f - \sigma_\mu}{\sigma_0}\Big)^m, \qquad \sigma_\mu = \alpha\mu b\sqrt{\rho}, \tag{1.4}$$

where α, u_0, and σ_0 are empirical constants, $m = H_0/(kT)$, H_0 is the characteristic activation energy, k is the Boltzmann constant, T is the temperature, and σ_μ is the stress caused by interaction of this dislocation with the closest neighborhood (stress of the third kind). At room temperature, the value for LiF is $m \approx 7$ [3]. The plastic shear strain rate $\dot\varepsilon$ is found by the Orowan–Taylor formula

$$\dot\varepsilon = b\rho u. \tag{1.5}$$

It follows from Eqs. (1.4) and (1.5) that plastic deformation begins if the inequality $\sigma > \sigma_*$ is satisfied ($\sigma_* = \sigma_f + \sigma_\mu$ is the critical shear stress). The dislocation velocity v in the direction perpendicular to the slip plane is determined by diffusion of point defects and vacancies to the dislocation [1]. There processes are not considered in the present work; hence, we assume that $v = 0$.

We assume that the main contribution to integration in Eqs. (1.2) is made by points x', y' close to x, y. Then we can assume that $u' \approx u(\rho)$, $\lambda_s' \approx \lambda_s(\rho)$, and $\rho = \rho(x, y)$ in Eq. (1.2), and the dislocation density can be presented as

$$\rho' \approx \rho + \frac{\partial\rho}{\partial x}\,(x' - x) + \frac{\partial\rho}{\partial y}\,(y' - y) + \frac{1}{2}\,\frac{\partial^2\rho}{\partial x^2}\,(x' - x)^2 + \frac{1}{2}\,\frac{\partial^2\rho}{\partial y^2}\,(y' - y)^2 + \frac{\partial^2\rho}{\partial x\,\partial y}\,(x' - x)(y' - y).$$

After calculating the integrals, we obtain the following system:

$$\frac{\partial\rho}{\partial t} + \frac{\partial\rho u}{\partial x} = D_x\,\frac{\partial^2\rho}{\partial x^2} + D_y\,\frac{\partial^2\rho}{\partial y^2} + f, \qquad \frac{\partial\rho_i}{\partial t} = \varphi,$$

$$D_x = q_{\mathrm{FR}} u\lambda_s \exp(-1/q), \qquad D_y = q_{\mathrm{FR}} u h_0^2 \chi(q)/(2\lambda_s),$$

$$\chi(q) = (1 + 2q + 2q^2)\exp(-1/q), \qquad q = h_c/h_0,$$

$$f = \rho u h_i(\rho_i^0 - \rho_i + n/(h_i\rho) + a\sqrt{\rho_f} - c\rho), \qquad \varphi = \rho u h_d(\rho_i^* - \rho_i), \tag{1.6}$$

$$\rho_i^* = \frac{1}{h_d\lambda_{ie}}, \qquad \rho_i^0 = \frac{1}{\lambda_q h_i}, \qquad a = \frac{\delta_f}{h_i}, \qquad c = \frac{h_a}{h_i}, \qquad \frac{1}{\lambda_q} = \frac{1}{\lambda_m} - \frac{1}{\lambda_{is}},$$

$$\frac{1}{\lambda_m} = \frac{q_{\mathrm{FR}}}{\lambda_s}\exp\Big(-\frac{1}{q}\Big), \qquad \frac{1}{\lambda_{ie}} = \frac{1}{\lambda_s}\Big(1 - \exp\Big(-\frac{1}{q}\Big)\Big).$$

Diffusion terms in the second equation of (1.6) are canceled, because the inequalities $D_x^i/D_x \ll 1$ and $D_y^i/D_y \ll 1$ are valid.

Equations (1.6) differ from the corresponding equations in [4] by the absence of the factor $1 - M$ in diffusion coefficients, where $M = -(\rho/u)\,\partial u/\partial\rho$. As $M \gg 1$ in most situations [4], the diffusion coefficients in [4] are negative, which contradicts the second law of thermodynamics and makes the well-posed formulation of the Cauchy problem impossible [8].

Let us find why the factor $1 - M$ appears in the corresponding equations of [4]. As was noted above, in calculating the integral in (1.2), the dislocation velocity was chosen at the mid-point $u' \approx u(\rho)$. To improve this approximation, Malygin [4] used the expansion into the series

$$u' \approx u + \frac{\partial u}{\partial\rho}\,\Delta\rho + \ldots = u\Big(1 - M\,\frac{\Delta\rho}{\rho}\Big) + \ldots\ , \tag{1.7}$$

where $\Delta\rho = \rho(x', y') - \rho(x, y)$; the dots indicate the terms of a higher order of smallness $O(\partial^2 u/\partial\rho^2(\Delta\rho)^2)$. We demonstrate that series (1.7) under given conditions is expanding. Differentiating formula (1.4), we obtain $\partial u/\partial\rho = -um\sigma_\mu/(2\rho(\sigma - \sigma_*))$. Then, the condition of convergence of series (1.7) — $M(\Delta\rho/\rho) < 1$ — is written as $m\sigma_\mu/(2(\sigma - \sigma_*))|\Delta\rho/\rho| < 1$, and the residual term has the order $O(m(m-1)(\sigma_\mu/(\sigma - \sigma_*)|\Delta\rho/\rho|)^2/2) < 1$. It follows from these inequalities that the series converges if the following inequality is satisfied:

$$\Big|\frac{\Delta\rho}{\rho}\Big| < \frac{2}{m}\,\frac{\sigma - \sigma_*}{\sigma_\mu}. \tag{1.8}$$

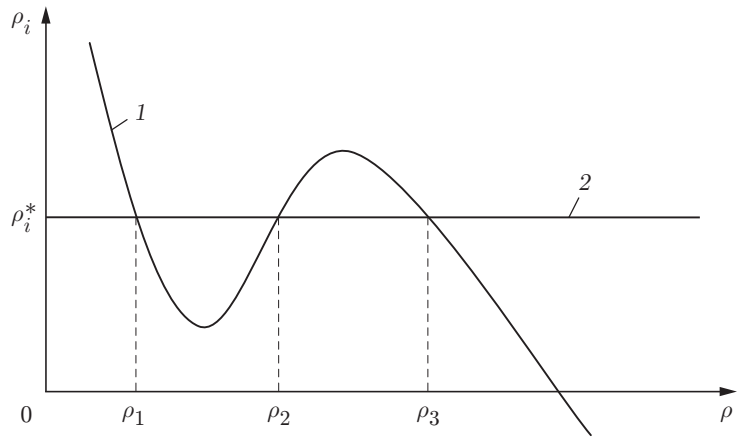

Fig. 2. Graphical solution of Eq. (2.1): curves 1 and 2 are described by the first and second equations in (2.1), respectively.

The main contribution to integral (1.2) is made by the distances $y' - y \simeq h_0 \simeq \mu b/(\sigma - \sigma_f)$; therefore, taking into account the symmetry of the integral kernel in (1.2), we obtain the estimate

$$\left|\frac{\Delta\rho}{\rho}\right| \simeq \frac{1}{2\rho}\,\frac{\partial^2\rho}{\partial y^2}\,(y'-y)^2 \simeq \frac{1}{2\rho}\,\frac{\partial^2\rho}{\partial y^2}\,\frac{\mu^2 b^2}{(\sigma-\sigma_f)^2}.$$

It follows from here that, for stresses tending to the shear stress ($\sigma \sim \sigma_* = \sigma_f + \sigma_\mu$), the right side in (1.8) tends to zero, the left side remains finite ($\sigma - \sigma_f = \sigma_\mu > 0$), and inequality (1.8) becomes invalid. In this case, series (1.7) diverges and cannot be used to calculate the integral in (1.2).

2. Analysis of Stability of the Steady Uniform Distribution of Dislocations. We find the steady uniform solution of (1.6) from the first two equations of system (1.6). Assuming that the derivatives with respect to time and coordinates in these equations are equal to zero and that $\rho_f \approx \rho$ for the density of forest dislocations, we reduce Eqs. (1.6) to two algebraic equations

$$\rho(\rho_i^0 - \rho_i) + n/h_i + a\rho^{3/2} - c\rho^2 = 0, \qquad \rho_i = \rho_i^*. \tag{2.1}$$

The roots of these equations ρ_1, ρ_2, and ρ_3 (Fig. 2) are found from the condition of intersection of curve 1 described by the first equation in (2.1) and curve 2 corresponding to the second equation in (2.1). The approximate values of the roots of system (2.1) are obtained by the formulas

$$\rho_1 \approx \frac{n}{h_i\Delta\rho_i}, \qquad \rho_2 \approx \left(\frac{\Delta\rho_i}{a}\right)^2, \qquad \rho_3 \approx \left(\frac{a}{c}\right)^2, \qquad \Delta\rho_i = \rho_i^* - \rho_i^0 > 0. \tag{2.2}$$

Let roots (2.2) satisfy the inequalities

$$\rho_1 \ll \rho_2 \ll \rho_3. \tag{2.3}$$

Then these roots are located far enough from the extreme points of curve 1 (see Fig. 2) and can be used in studying stability of the solutions of Eqs. (1.6). Inequalities (2.3) and the conditions of positiveness of the roots impose certain restrictions on the parameters in (1.6):

$$\Delta\rho_i > 0, \qquad \frac{na^2}{h_i\Delta\rho^3} \ll 1, \qquad \frac{\Delta\rho_i c}{a^2} \ll 1. \tag{2.4}$$

If inequalities (2.4) are satisfied, system (1.6) is structurally stable [9]. If the disturbances depend only on the variables t and x, the first two equations in (1.6) are written in the form

$$\frac{\partial\rho}{\partial t} = D_y\,\frac{\partial^2\rho}{\partial y^2} + f, \qquad \frac{d\rho_i}{dt} = \varphi \tag{2.5}$$

[the functions f, φ, and D_y are defined in (1.6)].

Introducing small deviations of dislocations from one of the roots (2.3) $\rho' = \rho - \rho_k$ or $\rho_i' = \rho_i - \rho_i^*$ ($k = 1, 2, 3$) as variables into Eqs. (2.5), we linearize Eqs. (2.5) in the neighborhood of ρ_k:

$$\frac{\partial\rho'}{\partial t} = a_{11}\rho' + a_{12}\rho_i' + D_y\frac{\partial^2\rho'}{\partial y^2}, \qquad \frac{\partial\rho_i'}{\partial t} = a_{21}\rho' + a_{22}\rho_i', \qquad a_{22} = -uh_d\rho_k,$$

$$a_{11} = uh_i(\rho_i^0 - \rho_i^* + (3/2)a\rho_k^{1/2} - 2c\rho_k), \qquad a_{12} = -uh_i\rho_k, \qquad a_{21} = 0. \tag{2.6}$$

Substituting the solution in the form $\rho' = \delta\rho\exp(pt+iky)$, $\rho_i' = \delta\rho_i\exp(pt+iky)$ into (2.6), we obtain the dispersion equation $(p + D_yk^2 - a_{11})(p - a_{22}) = 0$, which has the roots $p_1 = a_{11} - D_yk^2$ and $p_2 = a_{22}$. As $a_{22} < 0$, the root $p_2 < 0$ corresponds to the stable solution $\rho_i' \sim \exp(-|p_2|t)$. Using inequalities (2.4), we find the value of the root p_1 at singular points (2.2):

$$p_1 \approx -(uh_i\Delta\rho_i + D_yk^2) \qquad \text{for} \quad \rho = \rho_1,$$

$$p_1 \approx \frac{1}{2}\,uh_i\Delta\rho_i\Big(1 - 4\,\frac{c\Delta\rho_i}{a^2}\Big) - D_yk^2 \qquad \text{for} \quad \rho = \rho_2,$$

$$p_1 \approx -\Big(uh_i\,\frac{a^2}{2c} + D_yk^2\Big) \qquad \text{for} \quad \rho = \rho_3.$$

If diffusion is absent ($D_y = 0$), we have $p_1 < 0$ for $\rho = \rho_1$ or $\rho = \rho_3$ and $p_1 > 0$ for $\rho = \rho_2$; hence, the singular points (ρ_1, ρ_i^*) and (ρ_3, ρ_i^*) are stable nodes, and the point (ρ_2, ρ_i^*) is a saddle (see Fig. 2). Small perturbations in the neighborhood of the point (ρ_2, ρ_i^*) increase exponentially: $\rho' \sim \exp(p_1t)$. If diffusion is taken into account, increasing perturbations have the wave vectors $k < \sqrt{uh_i\Delta\rho_i(1 - 4c\Delta\rho_i/a^2)/(2D_y)}$ and the wavelength

$$\lambda > \lambda_{\min}, \qquad \lambda_{\min} = h_0\sqrt{\frac{2}{3}\,\frac{q_{\rm FR}\lambda_m\chi(q)}{\lambda_s(\beta_i - 1)}}, \qquad \beta_i = \frac{h_i\lambda_m}{h_d\lambda ie} + \frac{\lambda_m}{\lambda_{is}}. \tag{2.7}$$

[In (2.7), we use the formula $\Delta\rho_i = (\beta_i - 1)/(h_i\lambda_m) > 0$.] Let us estimate $\lambda_{\min}$ for a LiF crystal loaded by the shear stress $\sigma = 5$ MPa. Assuming in (2.7) that $\beta_i = 2$, $q_{\rm FR} = 1$, $q = 1/2$, $\nu = 0.25$, $\sigma_f = 1$ MPa, $b = 0.3$ nm, and $\mu = 4.3 \cdot 10^4$ MPa, we obtain $\lambda_{\min} \approx h_0 \approx 170$ nm. Our analysis shows that the steady uniform state (ρ_2, ρ_i^*) is unstable to small perturbations, whereas two other states are stable.

We consider a constant-section sample (see Fig. 1) extended along its axis, so that the shear stress σ acts in the slip plane. If the inequality $\sigma > \sigma_f + \sigma_\mu$ is satisfied, the sources of dislocations in some slip planes are activated. Using the above-formulated mathematical model (1.6), we study the development of plastic deformation in the LiF single crystal. We assume that the loaded single crystal is in the stable state (ρ_1, ρ_i^*), and the Frank–Reed source emits a finite number of dislocations N in a certain slip plane. We consider the problem of evolution of this finite disturbance.

Introducing the variables

$$\tilde y = y\sqrt{\rho_3}, \quad \tilde t = \frac{t}{T}, \quad T = \frac{1}{u_wh_a\rho_3}, \quad \tilde\rho = \frac{\rho}{\rho_3}, \quad \tilde\rho_i = \frac{\rho_i}{\rho_3}, \quad \rho_{23} = \frac{\rho_2}{\rho_3},$$

$$\tilde u = \frac{u}{u_w} = \Big(\frac{1 - \sigma_f/\sigma - \sqrt{\tilde\rho}\,\sigma_d/\sigma}{1 - \sigma_f/\sigma - \sqrt{\tilde\rho_w}\,\sigma_d/\sigma}\Big)^m,$$

we write Eqs. (2.5) in dimensionless form

$$\frac{\partial\tilde\rho}{\partial\tilde t} = \tilde D\,\frac{\partial^2\tilde\rho}{\partial\tilde y^2} + \tilde f, \qquad \frac{\partial\tilde\rho_i}{\partial\tilde t} = \tilde\varphi,$$

$$\tilde D = \frac{q_{\rm FR}\tilde uh_0^2}{2\lambda_sh_a}\,\chi(q), \qquad \tilde f = -\tilde u\tilde\rho(\sqrt{\tilde\rho} - \sqrt{\rho_{23}})(\sqrt{\tilde\rho} - 1), \tag{2.8}$$

$$\tilde\varphi = \tilde\rho\tilde u\,\frac{h_d}{h_a}\,(\tilde\rho_i^* - \tilde\rho_i), \qquad \dot{\tilde\varepsilon} = \frac{\tilde b\tilde\rho\tilde u}{h_a\sqrt{\rho_3}}, \qquad \varepsilon = \int\limits_0^{\tilde t}\dot{\tilde\varepsilon}\,d\tilde t,$$

where ρ_w is the characteristic density of moving dislocations and u_w and σ_d are the characteristic velocities and stresses determined by the formulas

$$\sigma_d = \sigma_\mu(\rho_3), \qquad u_w = u_0((\sigma - \sigma_f - \sigma_\mu(\rho_w))/\sigma_0)^m. \tag{2.9}$$

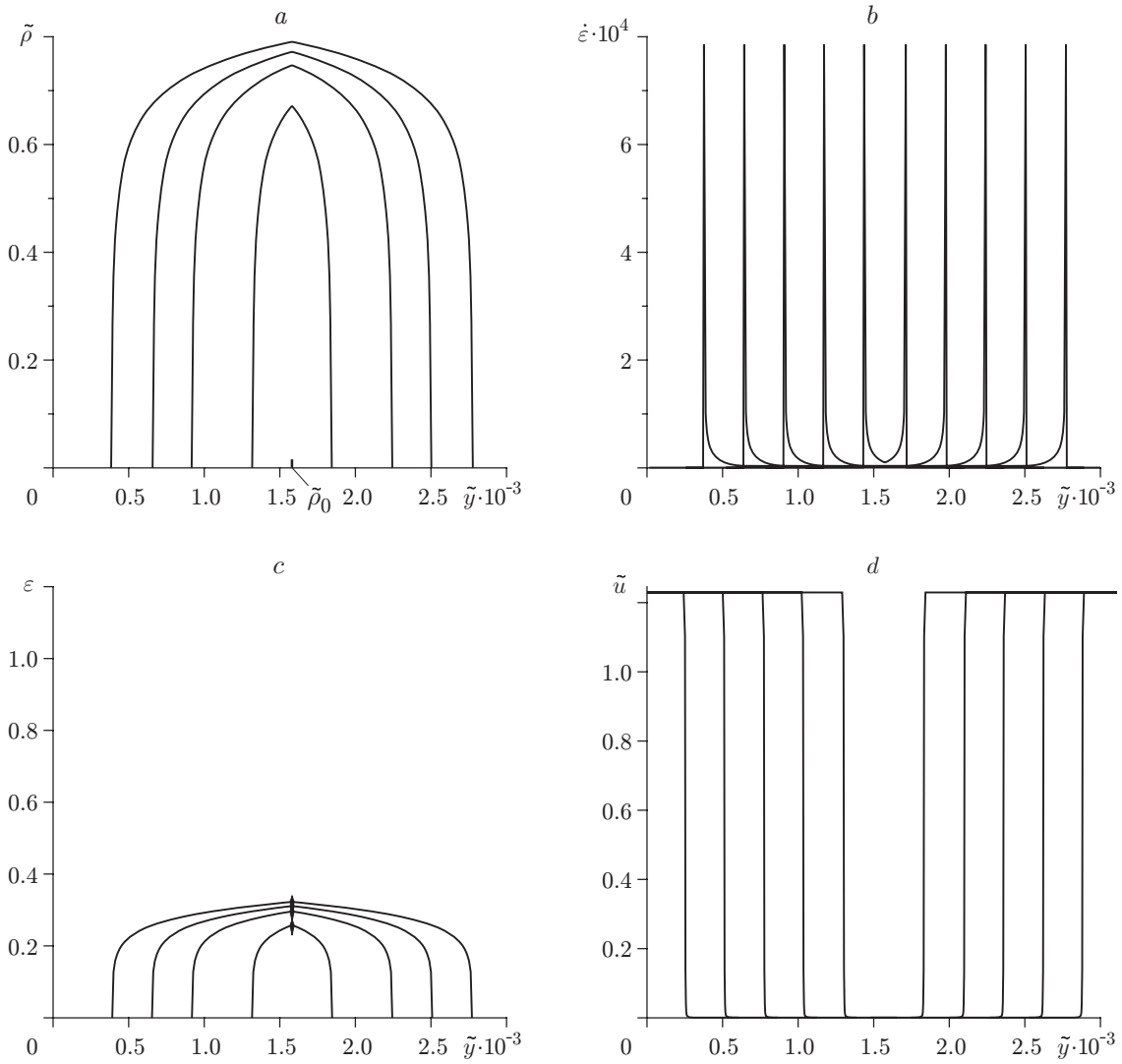

Fig. 3. Results of the numerical solution of Eqs. (1.4) and (2.8) for $\sigma = 2.3$ MPa at different times: (a) dislocation density; (b) plastic strain rate; (c) plastic strain; (d) dislocation velocity; $\tilde\rho_0$ is the initial perturbation of dislocation density.

Sample deformation involves turning of the main axes of the stress tensor by an angle $\delta\psi = \varepsilon$ with respect to the slip plane of dislocations (see Fig. 1). This alters the shear stress in the slip plane; therefore, the stress σ in the formulas (1.4) and (2.9) for the dislocation velocity has to be replaced by $\sigma' = \sigma \sin(\pi/2 + 2\varepsilon)$. This correction is important because Eq. (1.4) predicts that the dislocation velocity is a rapidly changing function of the shear stress σ.

The solution of system (2.8) is sought in the domain $0 < \tilde y < \tilde L$, $t > 0$. As the initial conditions, we use the stable state $\tilde\rho = \tilde\rho_1$ and $\tilde\rho_i = \tilde\rho_i^*$ for $0 < \tilde y < \tilde L_1$ and $\tilde L_1 + \Delta H < \tilde y < \tilde L$ and the perturbed state $\tilde\rho = \tilde\rho_1 + \Delta\tilde\rho$ on the segment $\tilde L_1 < \tilde y < \tilde L_1 + \Delta\tilde H$. The domain boundaries $\tilde y = 0$ and $\tilde y = \tilde L$ are subjected to the conditions $\tilde\rho = \tilde\rho_1$ and $\tilde\rho_i = \tilde\rho_i^*$. Equations (2.8) were solved numerically by a second-order explicit scheme, which is described, e.g., in [10]. The numerical calculations were performed with the use of the following parameters: $\tilde\rho_1 = 0$, $\tilde\rho_2 = 0.01$, $\tilde\rho_3 = 1$, $\Delta\tilde\rho = 0.02$, $\tilde\rho_w = 10^{-3}$, $\Delta\tilde H = 4$, $\tilde L_1 = 1750$, $\tilde L = 3200$, and $\sigma = 2.3$ MPa. The parameters used for the LiF single crystal were $\mu = 4.3 \cdot 10^4$ MPa, $\nu = 0.35$, $b = 3 \cdot 10^{-10}$ m, $\lambda_s = 1.3 \cdot 10^{-3}$ m, $h_a = 5 \cdot 10^{-9}$ m, $m = 8$, $\chi(q) = 1$, $\sigma_f = 1.3$ MPa, $\sigma_0 = 5$ MPa, $\alpha = 0.3$, $u_0 = 2 \cdot 10^3$ m/sec, and $q_{\rm FR} = 2$.

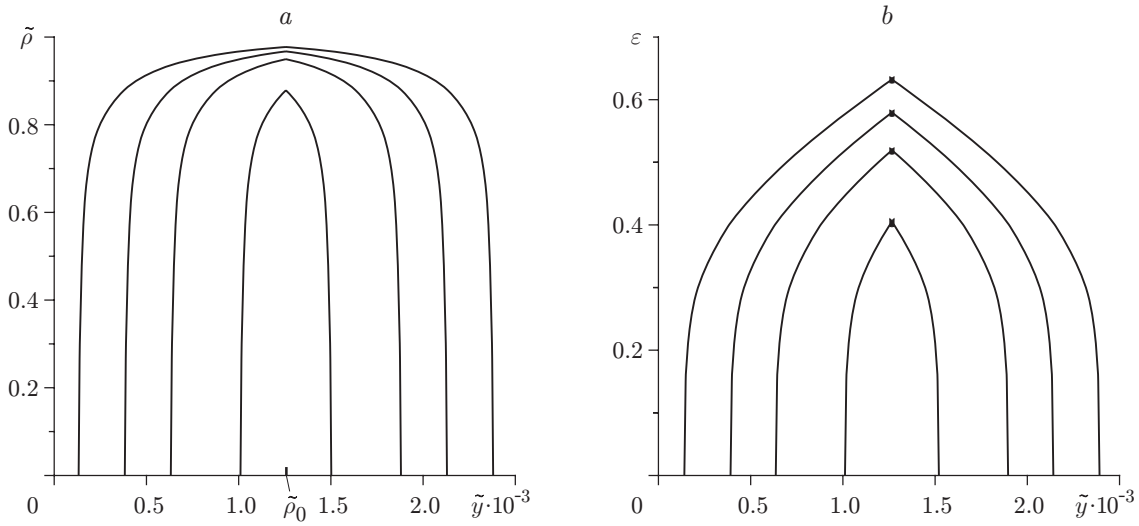

Fig. 4. Results of the numerical solution of Eqs. (1.4) and (2.8) for $\sigma = 2.5$ MPa at different times: (a) dislocation density; (b) plastic strain .

The dislocation density, strain rate, plastic strain, and dislocation velocity calculated for several time instants as functions of the coordinate y are plotted in Fig. 3a–d, respectively. During the time $\Delta\tilde t = 6.7\cdot 10^3$ ($T = 0.22$ sec), the initial perturbation increases to $\tilde\rho = 0.65$ and generates waves propagating to the left and to the right from the source of perturbations. The wave parameters first change with time, then the process becomes stabilized, and each wave propagates with a constant velocity. The deformation occurs in the wave front (Fig. 3b), and the strain is almost constant behind the front (Fig. 3c). The reason is a rapid deceleration of dislocations behind the wave front owing to internal stresses σ_μ (1.4), and the dislocation velocity vanishes (Fig. 3d). The region between the fronts of two waves propagating in the opposite directions can be interpreted as a shear band expanding with a constant velocity. The solution obtained is in qualitative agreement with the experimental data [3] according to which the entire deformation occurs in the band front. (For a quantitative comparison, one has to calculate the stress-strain state of the sample, which varies significantly in the course of deformation.) If the amplitude of the initial perturbation does not cross the unstable point $\Delta\tilde\rho < \tilde\rho_2$, this perturbation decays, and no waves are observed.

For high values of stress $\sigma = 2.5$ MPa, the calculations also predict the existence of two abrupt fronts, which propagate with a constant velocity in the opposite directions at high times (Fig. 4). In this case, however, the strain rate differs from zero not only in the wave front but also in the entire perturbed region. The strain increases linearly in the direction from the wave front to the band center (Fig. 4b). This solution can be interpreted as strain localization, which occurs owing to an increase in stress in the region of evolution of the shear band.

3. Solution of the Traveling-Wave Type. We construct the solution of Eqs. (2.5) in the class of traveling waves. If the density of motionless dislocations is constant ($\partial\rho_i/\partial t = 0$) and the concentration of the Frank–Reed sources is low ($n \to 0$), Eq. (2.5) yields the following equation of the type of the Kolmogorov–Petrovskii–Piskunov–Fisher equation:

$$\frac{\partial\rho}{\partial t} = D_y\,\frac{d^2\rho}{dy^2} + f, \qquad f = uh_i(a\rho^{3/2} - \Delta\rho_i\rho - c\rho^2), \qquad \rho_i = \rho_i^* \tag{3.1}$$

[the dislocation velocity $u = u(\rho)$ is defined in Eq. (1.4)]. This equation is known to have a solution in the form of a switching traveling wave, which converts one steady solution to another [9]. Choosing the solutions ρ_1 and ρ_3 from (2.2) as steady solution, we seek for the solution of (3.1) in the form

$$\rho = \rho(\zeta), \qquad \zeta = y - Ut, \tag{3.2}$$

which satisfies the boundary conditions

$$\rho = \rho_1 = 0 \quad \text{as} \quad \zeta \to \infty, \qquad \rho = \rho_3 \quad \text{as} \quad \zeta \to -\infty. \tag{3.3}$$

Substituting (3.2) into the first equation in (3.1), we obtain

$$D_y \frac{d^2\rho}{d\zeta^2} + U \frac{d\rho}{d\zeta} + f = 0. \tag{3.4}$$

Karlov and Kirichenko [9] described the solution of Eq. (3.4) with a constant diffusion coefficient $D_y = \text{const}$ and a function $f = \psi(\rho) = \beta\rho + \varepsilon\rho^2 - \rho^3$. As the argument changes, the character of the dependence $\psi(\rho)$ is similar to the character of the dependence of the function $f(\rho)$ in (3.1); therefore, the corresponding solutions are similar.

We present Eq. (3.4) as a system of two first-order equations

$$\frac{d\rho}{d\zeta} = w, \qquad \frac{dw}{d\zeta} = -\frac{f + Uw}{D_y}. \tag{3.5}$$

From the algebraic equations $f + Uw = 0$ and $w = 0$, we find the singular points ρ_1, ρ_2, and ρ_3 of system (3.5), where $\rho_1 = 0$, and the values of ρ_2 and ρ_3 are defined by formulas (2.2). Expanding the function $f(\rho)$ into a series in the neighborhood of the singular points ρ_k and presenting the solution of system (3.5) in the form $\rho - \rho_k = a_1 \exp(\lambda\zeta)$, $w = a_2 \exp(\lambda\zeta)$, we find the eigenvalues

$$\lambda_{1,2} = -g_2/2 \pm \sqrt{g_2^2/4 + g_1}, \qquad g_1 = \omega(\rho_k)/D_y(\rho_k), \quad g_2 = U/D_y(\rho_k) \quad (k = 1, 3)$$

at the points ρ_1 and ρ_3, and

$$\lambda_{1,2} = -g_2/2 \pm \sqrt{g_2^2/4 - g_1} \qquad [g_1 = \omega(\rho_2)/D_y(\rho_2), \quad g_2 = U/D_y(\rho_2)]$$

at the point ρ_2. Here $\omega(\rho_1) = u(\rho_1)h_i c\sqrt{\rho_2\rho_3} > 0$, $\omega(\rho_2) = (1/2)u(\rho_2)h_i c\sqrt{\rho_2}\,(\sqrt{\rho_3} - \sqrt{\rho_2}) > 0$, and $\omega(\rho_3) = (1/2)u(\rho_3)h_i c\sqrt{\rho_3}\,(\sqrt{\rho_3} - \sqrt{\rho_2}) > 0$. It follows from here that the eigenvalues at the points ρ_1 and ρ_3 have different signs ($\lambda_1 < 0$ and $\lambda_2 > 0$ for $U > 0$); therefore, the points ρ_1 and ρ_3 are saddles. The character of the singular point ρ_2 depends on the wave velocity U: it is a node for $g_2^2 > 4g_1$ and a focus for $g_2^2 < 4g_1$. If the point ρ_2 is a node, it is impossible to pass from the point ρ_1 to the point ρ_3; if the point ρ_2 is a focus, there exists a unique value of the velocity U that allows a continuous path from the point ρ_1 to the point ρ_3 along the separatrix. The choice of the sign of U is determined from the condition that the system passes to a state with the least "potential energy" $-V(\rho) = -\int f(\rho)\,d\rho$ [9], which, in our case, is equal to

$$-V(\rho) = uh_i\rho(\Delta\bar{\rho}_i\rho - \bar{a}\rho^{3/2} + \bar{c}\rho^2), \qquad \Delta\bar{\rho}_i = \Delta\rho_i/2, \quad \bar{a} = 2a/5, \quad \bar{c} = c/3.$$

As we have ($\rho_1 = 0$) $-V(\rho_1) = 0$ in the first stable steady state and ($\rho_3 = (a/c)^2$) $-V(\rho_3) = -(4/15)uh_i a(a/c)^5 < 0$ in the second stable steady state, the transition from the state ρ_1 to the state ρ_3 occurs in the switching wave, and the wave propagates to the left ($U > 0$). In this case, in contrast to [9], it is impossible to construct the exact solution of Eq. (3.4). At high stresses ($\sigma \gg \sigma_f + \sigma_\mu$), however, where the dependence of the dislocation velocity on the dislocation density can be neglected, such a solution does exist. Introducing the dimensionless coordinates

$$\tilde{\zeta} = \zeta\sqrt{\rho_3}, \qquad \tilde{\rho} = \rho/\rho_3, \qquad \tilde{U} = U/(uh_a\sqrt{\rho_3})$$

and assuming that $u = \text{const}$, we write Eq. (3.4) in the form

$$\tilde{A}\frac{d^2\tilde{\rho}}{d\tilde{\zeta}^2} + \tilde{U}\frac{d\tilde{\rho}}{d\tilde{\zeta}} + f = 0, \qquad f = -\tilde{\rho}\Big(\sqrt{\tilde{\rho}} - \sqrt{\frac{\rho_2}{\rho_3}}\Big)(\sqrt{\tilde{\rho}} - 1), \quad \tilde{A} = \frac{D_y}{uh_a}, \tag{3.6}$$

where ρ_2 and ρ_3 are the roots of the equation $f = \rho(a\sqrt{\rho} - \Delta\rho_i - c\rho) = 0$:

$$\rho_{2,3} = (a/(2c) \mp \sqrt{G})^2, \qquad G = (a/(2c))^2 - \Delta\rho_i/c.$$

Writing the boundary conditions (3.3) in the dimensionless variables

$$\tilde{\rho} \to 0 \quad \text{at} \quad \tilde{\zeta} \to \infty, \qquad \tilde{\rho} \to 1 \quad \text{at} \quad \tilde{\zeta} \to -\infty,$$

we obtain the solution of Eq. (3.6) in the form

$$\tilde{\rho} = 1/(1 + \exp(\tilde{\zeta}/\delta))^2, \qquad \tilde{U} = \sqrt{6\tilde{A}}\,(\sqrt{G/\rho_3} - 1/6), \qquad \delta = \sqrt{6\tilde{A}}. \tag{3.7}$$

Figure 5 shows the results of the numerical solution of the ordinary differential equations (3.5) and (3.6) in the phase plane $w = d\tilde{\rho}/d\tilde{\zeta}$, $\tilde{\rho}$ for $A = 1$, $\tilde{\rho}_2/\tilde{\rho}_3 = 0.2$, and different values of the wave velocity U (the tilde

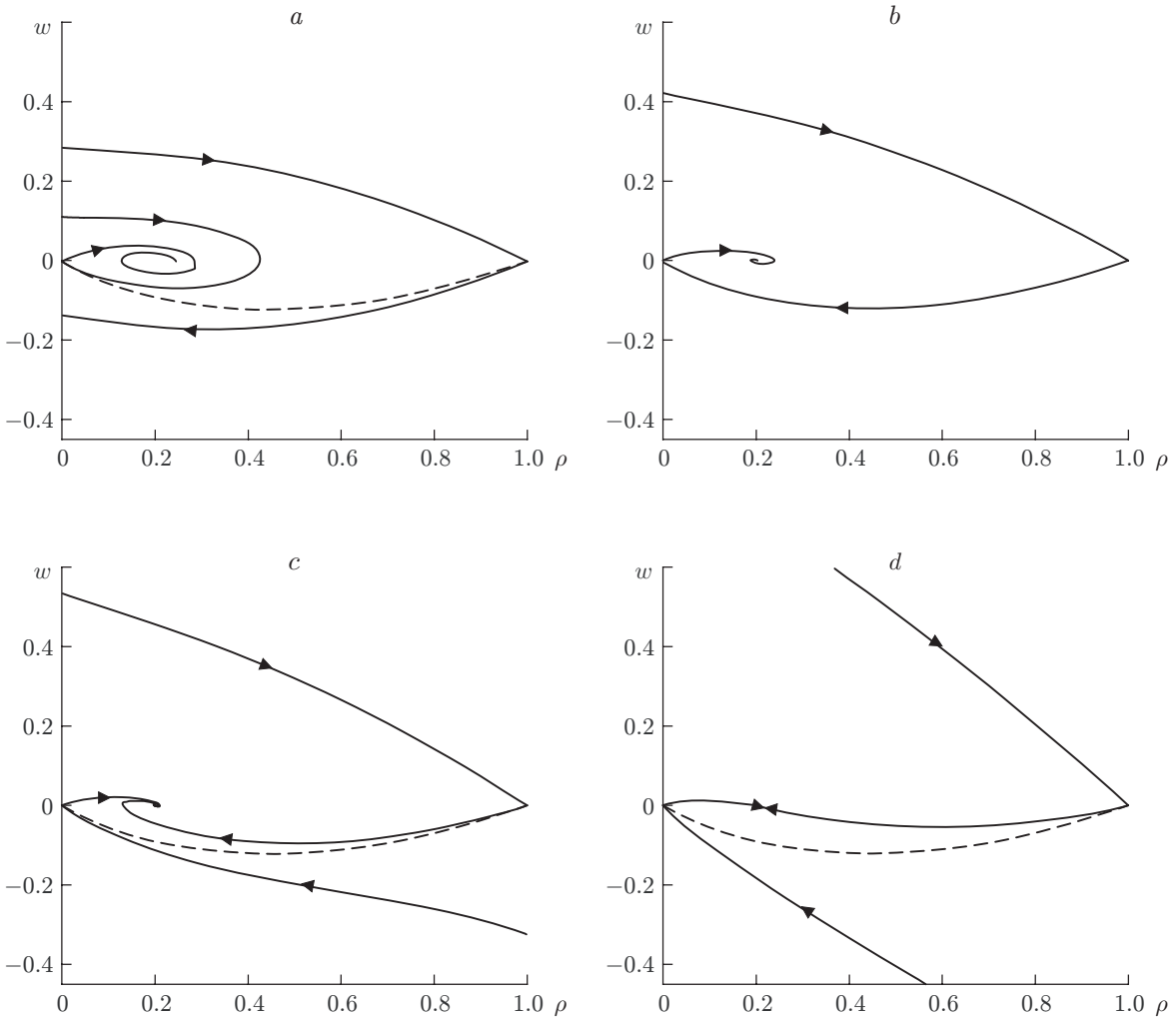

Fig. 5. Integral curves of system (3.5) in the phase plane $w = d\tilde{\rho}/d\tilde{\zeta}$, $\tilde{\rho}$ for $U = 0.1$ (a), 0.262 (b), 0.4 (c), and 0.8 (d); the dashed curve is the exact solution of Eq. (3.7).

above the dimensionless quantities is omitted in Fig. 5). The dashed curve shows the exact solution of Eq. (3.7) $w = -2\tilde{\rho}(1 - \sqrt{\tilde{\rho}})/\sqrt{6\tilde{A}}$ in the phase plane w, ρ. The calculated behavior of integral curves for different values of the wave velocity U is consistent with the results of the above-performed qualitative analysis of the solution of system (3.5). For $U = 0.1$ and 0.4, the singular point $\tilde{\rho}_2 = 0.2$ is a focus capturing integral curves emanating from the point $\tilde{\rho}_1 = 0$ (Fig. 5a) or from the point $\tilde{\rho}_3 = 1$ (Fig. 5c). For $U = 0.8$, the point $\tilde{\rho}_2 = 0.2$ is a stable node simultaneously capturing two integral curves emanating from the points $\tilde{\rho}_1 = 0$ and $\tilde{\rho}_3 = 1$ (Fig. 5d). It is only the value $U = 0.262$ that ensures the existence of a continuous integral curve (separatrix) connecting the initial state ($\tilde{\rho}_1 = 0$) and final state ($\tilde{\rho}_3 = 1$) (see Fig. 5b). This value $U = 0.262$ equals the velocity of the traveling wave.

In the general case of a variable dislocation velocity, a solution of the traveling-wave type can be obtained by solving system (2.8), (1.4) numerically in the domain $0 < \tilde{\zeta} < 1$ with appropriate boundary conditions. The solution obtained in calculations is similar to the solutions plotted in Figs. 3 and 4, where the point of the maximum dislocation density has to be shifted to the origin, and only one wave traveling either to the right or to the left has to be considered. In contrast to the exact solution of Eq. (3.7), the maximum dislocation density in the numerical solution plotted in Fig. 3a is smaller than unity. The reason is the dependence of the dislocation velocity on density (1.4), which implies that the dislocation velocity equals zero for the density $\rho_4 = ((\sigma - \sigma_f)/(\alpha\mu b))^2$. In this case, the right sides of Eqs. (2.5) and (2.8) vanish, which yields another steady solution in addition to (2.2): $\partial\rho/\partial t = \partial\rho_i/\partial t = 0$, where $\rho = \rho_4$. [As the first equation in Eqs. (2.5) and (2.8) was divided by the second

equation, the velocity was canceled out, and this solution was lost in obtaining the steady solutions of (2.2).] If the inequality $\tilde{\rho}_4 < 1$ holds, the solution shown in Fig. 3 with the maximum dislocation density $\tilde{\rho}_{\max} = \tilde{\rho}_4$ ($\tilde{\rho}_4 = \rho_4/\rho_3$) is obtained. Otherwise ($\tilde{\rho}_4 > 1$), the solution plotted in Fig. 4 with the maximum dislocation density $\tilde{\rho}_{\max} = 1$ is obtained.

Conclusions. A mathematical model of the development of plastic deformation owing to the mechanism of double cross-slips is proposed. A solution of the traveling-wave type is constructed, and its structure is considered. The stability of the uniform state of the single crystal is examined. It is shown that the perturbation entering an unstable region increases, and two shear bands propagate in the opposite directions, each of them being described by a solution of the traveling-wave type. Two types of solutions depending on the magnitude of the applied stress are possible. For low stresses, plastic deformation occurs in the shear-band front, and the strain remains constant behind the wave front. At high stresses, the strain rate behind the wave front differs from zero, and the strain linearly increases with distance from the wave front. The calculated results are in qualitative agreement with experimental data.

This work was partly supported by the Russian Foundation for Basic Research (Grant No. 04-01-00894a).

REFERENCES

1. J. Friedel, *Dislocations*, Pergamon Press, Oxford–New York (1967).
2. A. Ziegenbein, J. Plessing, and H. Neuhäuser, "Mesoscale studies on Lüders band deformation in concentrated Cu-based alloy single crystals," *Phys. Mesomech.* **1**, No. 2 (1998).
3. B. I. Smirnov, *Dislocation Structure and Hardening of Crystals* [in Russian], Nauka, Leningrad (1981).
4. G. A. Malygin, "Self-organization of dislocations and plasticity of crystals," *Usp. Fiz. Nauk*, **169**, No. 9, 979–1010 (1999).
5. P. Hahner, "Theory of solitary plastic waves. 1. Lüders bands in polycrystals," *Appl. Phys., A*, **58**, 41–48 (1994).
6. P. Hahner, "Theory of solitary plastic waves. 2. Lüders bands in single glide-oriented crystals," *Appl. Phys., A*, **58**, 49–58 (1994).
7. S. P. Kiselev, "Internal stresses in a solid with dislocations," *J. Appl. Mech. Tech. Phys.*, **45**, No. 4, 567–571 (2004).
8. S. K. Godunov and E. I. Romensky, *Elements of Continuum Mechanics and Conservation Laws*, Kluwer Acad. Publ., Dordrecht (2003).
9. N. V. Karlov and N. A. Kirichenko, *Oscillations, Waves, and Structures* [in Russian], Fizmatlit, Moscow (2001).
10. S. K. Godunov and V. S. Ryaben'kij, "Difference schemes. An introduction to the underlying theory," in: *Studies in Mathematics and Its Applications*, Vol. 19, North-Holland, Amsterdam (1987).